Collective dynamics in binary liquids: spectra dependence on mass ratio

2005 J. Phys.: Condens. Matter 17 413

(http://iopscience.iop.org/0953-8984/17/3/002)

INSTITUTE OF PHYSICS PUBLISHING JOURNAL OF PHYSICS: CONDENSED MATTER

J. Phys.: Condens. Matter **17** (2005) 413–427 doi:10.1088/0953-8984/17/3/002

Collective dynamics in binary liquids: spectra dependence on mass ratio

Taras Bryk and Ihor Mryglod

Institute for Condensed Matter Physics, National Academy of Sciences of Ukraine, 1 Svientsitskii Street, UA-79011 Lviv, Ukraine

Received 16 July 2004, in final form 31 October 2004
Published 7 January 2005
Online at stacks.iop.org/JPhysCM/17/413

Abstract

We discuss the spectrum of longitudinal propagating collective excitations in a liquid metallic alloy Li_4Pb and a Lennard-Jones binary mixture obtained by an eight-variable approach of generalized collective modes. Reported wavenumber-dependent amplitudes of contributions from high- and low-frequency propagating excitations to dynamical structure factors in Li_4Pb permit a new viewpoint on the 'fast sound' phenomenon. A three-variable analytical model for slow and fast mass–concentration fluctuations is used for explanation of the high-frequency branch in the long-wavelength region. An additional analysis of longitudinal dynamics in liquid binary mixtures with different mass ratio of components permits us to establish a tendency in frequency and damping coefficients of the high-frequency propagating excitations.

1. Introduction

Collective dynamics in liquids is a challenging problem of modern statistical physics. So far the hydrodynamic approach remains the only reliable theoretical model; it yields analytical expressions for time correlation functions and dynamical eigenmodes, although it is valid only in the limit of small wavenumbers k and frequencies ω. For binary liquids the dominant dynamical processes that determine the collective dynamics beyond the hydrodynamic region are still under discussion. For the longitudinal dynamics it is generally accepted that there exist at least two branches of propagating excitations beyond the hydrodynamic region, which in the short-wavelength region describe the partial dynamics of heavy and light components in a binary liquid mixture. However, regarding the dispersion laws of these two branches by approaching the hydrodynamic region there is no clear model for describing the crossover in dispersion from the molecular region to the hydrodynamic one. Especially big problems arise for mixtures composed of disparate mass particles—up to date it is not finally established what is going on with the high-frequency propagating branch in the long-wavelength limit. Hence,

the problem of 'fast sound' [1] reported over almost 20 years in the literature for the case of a metallic melt Li_4Pb is still far from being finally solved. It is also not known what the role of concentration is in the damping coefficients of high-frequency branch, how the mass ratio affects the width of hydrodynamic region, or how the dispersion law will change by decreasing the concentration of relevant species down to the impurity limit.

One of the most natural ways for exploring the collective dynamics in binary liquids is to apply as much as possible simple theoretical models and reliable schemes for analysis of computer experiments in order to clarify the dominant relaxing and propagating processes in a wide range of wavenumbers and frequencies, including the hydrodynamic region. One of the most promising schemes for analysis of the collective dynamics in liquids is a parameter-free approach of generalized collective modes (GCM) [2], which combines molecular dynamics (MD) simulations with the eigenvalue problem for a generalized hydrodynamic matrix [3, 4]. Recently, the simplest dynamical processes in the transverse dynamics of a binary equimolar liquid KrAr [5, 6] were studied using the GCM approach. A clear picture of transverse dynamics in terms of two branches of propagating excitations was obtained: in the short-wavelength region the branches have partial character describing the dynamics of light and heavy components, while on approaching the long-wavelength region the low-frequency branch obeys the shear wave dispersion law with a propagation gap in the $k \to 0$ limit and high-frequency branch describes optic phonon-like excitations. A simple theoretical model for separated transverse mass–concentration current fluctuations permitted the origin of the optic-like branch in the long-wavelength limit to be explained, and light to be shed on the physical processes causing the damping of transverse optic-like excitations [5, 6]. Later a similar three-variable dynamical model of mass–concentration fluctuations was solved analytically in the long-wavelength limit for the case of longitudinal dynamics [7]. It was remarkable that for the longitudinal case exactly the same mechanism of damping for the optic-like excitations was obtained. It was shown that high mutual diffusion and the tendency to demixing when the atoms are mainly surrounded by like particles cause strong damping of optic-like excitations and can even suppress them. Such a mechanism of suppressing the optic-like propagating branch seems to work in a gaseous mixture $He_{0.65}Ne_{0.35}$ [4, 7], where on approaching the small-k region the high-frequency branch vanishes from the spectrum.

Thus, the eigenmode analysis clearly indicates that in the long-wavelength region there must exist an optic-like branch of mass–concentration waves unless some specific processes in the liquid (like high diffusion or demixing tendency) suppress it. However, in the literature there exists a number of reports on dispersion curves in binary liquids estimated numerically from partial current spectral functions $C_{\alpha\alpha}(k, \omega)$, $\alpha = A, B$ obtained in MD [8–11], and the general picture of dispersion curves obtained in these studies is a merger of two branches, high- and low-frequency ones, on approaching the long-wavelength region, into a single branch with linear dispersion corresponding to hydrodynamic sound. In figure 1, we show that for the equimolar Lennard-Jones KrAr liquid mixture the spectrum of propagating excitations obtained numerically from the maxima positions of partial spectral functions $C_{\alpha\alpha}(k, \omega)$, $\alpha =$ Kr, Ar, is very similar to these results [8–11]. Hence, even for the case of small mass ratio ($R = 2.098$ for KrAr) following the *numerical* results there is a temptation to talk about 'fast sound modes', while the *analytical* parameter-free GCM analysis of eigenmodes in liquid KrAr [7] clearly gives two kinds of propagating solutions in long-wavelength region: hydrodynamic sound and kinetic optic phonon-like excitations. The latter have finite damping coefficient in the long-wavelength limit and therefore their contributions to $C_{\alpha\alpha}(k, \omega)$ become extremely small in comparison with contributions from hydrodynamic modes in the $k \to 0$ limit.

The goal of this study is to obtain the spectrum of collective propagating eigenmodes in the liquid metallic 'fast sound' alloy Li_4Pb and analyse its high-frequency branch. The

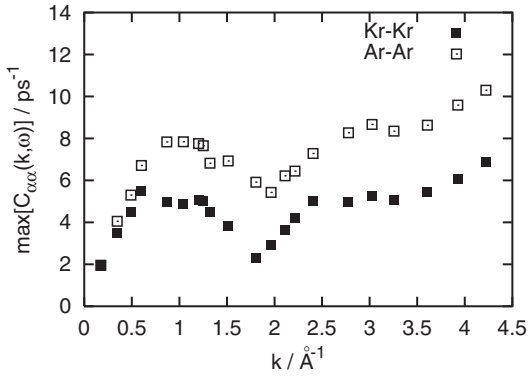

Figure 1. Maxima positions of partial spectral functions $C_{\alpha\alpha}(k,\omega)$, ($\alpha$ = Kr, Ar) against wavenumber for a Lennard-Jones equimolar liquid KrAr at 116 K.

dependence of frequency and damping coefficients for high-frequency excitations on the mass ratio of the components will be discussed with an example of a GCM study of Lennard-Jones liquid mixtures. The remaining part of the paper is organized as follows. In section 2 we describe the basic ideas of the GCM approach and give details of our MD simulations. In section 3 we present the numerical results, obtained for Li_4Pb and Lennard-Jones liquid mixtures within the eight-variable GCM approach. The dependence of frequency and damping of optic-like excitations on mass ratio will be discussed in section 4 using an analytical solution for a three-variable dynamical model, and the following section contains our conclusions of this study.

2. Method

2.1. Approach of generalized collective modes

The approach of generalized collective modes consists of solving the generalized Langevin equation in matrix form in terms of dynamical eigenmodes. For a chosen basis set of N_v dynamical variables a generalized hydrodynamic matrix $\mathbf{T}(k)$ in Markovian approximation reads (see [3, 4] for details of the GCM approach)

$$\mathbf{T}(k) = \mathbf{F}(k, t = 0)\tilde{\mathbf{F}}^{-1}(k, z = 0), \tag{1}$$

where $\mathbf{F}(k,t)$ and $\tilde{\mathbf{F}}(k,z)$ are the $N_v \times N_v$ matrices of time correlation functions and their Laplace transforms, respectively. Usually the basis set of dynamical variables for binary liquids is constructed from the hydrodynamic set of four variables (in the case of longitudinal dynamics of a binary liquid) by extending it with more short-time dynamical variables, which describe orthogonal processes (in the sense of thermodynamic fluctuation theory) to hydrodynamic ones. Such extended dynamical variables are usually represented by time derivatives of the hydrodynamic variables. Among the N_v eigenmodes the lowest four correspond in the long-wavelength region to hydrodynamic modes, while the other $N_v - 4$ describe kinetic collective propagating or relaxing processes with finite nonzero damping coefficient in the $k \to 0$ limit. The eigenvalues and eigenvectors of the generalized hydrodynamic matrix $\mathbf{T}(k)$ permit the calculation of GCM-replicas of the relevant time correlation functions via [12]

$$F^{\mathrm{GCM}}_{\alpha\beta}(k,t) = \sum_{j=1}^{N_v} G^{j}_{\alpha\beta}(k)\mathrm{e}^{-z_j(k)t}, \tag{2}$$

with the eigenvalues $z_j(k)$ and weight coefficients $G^j_{\alpha\beta}(k)$ defining the contribution of each generalized collective mode to the time correlation function. Note that for the hydrodynamic basis set of four/three variables in the case of longitudinal dynamics in binary/pure liquids the expressions (1) and (2) have exactly the hydrodynamic form [13]. For the case of an extended basis set with short-time dynamical variables in addition to hydrodynamic ones these expressions represent the generalization of hydrodynamics onto the case of existence of kinetic collective excitations in the liquid with finite lifetime, that is supposed to represent correctly the shape of the relevant time correlation functions (and dynamical structure factors) beyond the hydrodynamic region.

A connection between the GCM approach and experimentally accessible quantities is made via the expression for a set of dynamical structure factors

$$\frac{S_{\alpha\beta}(k,\omega)}{S_{\alpha\beta}(k)} = \sum_{j}^{N_{\rm r}} A^j_{\alpha\beta}\frac{d_j(k)}{\omega^2+d_j^2(k)} + \sum_{j,\pm}^{N_{\rm p}} \frac{B^j_{\alpha\beta}\sigma_j(k) + D^j_{\alpha\beta}(\omega \pm \omega_j(k))}{(\omega \pm \omega_j(k))^2+\sigma_j^2(k)}, \qquad \alpha,\beta = \{a_i(k,t)\}, \tag{3}$$

which generalizes the four-term hydrodynamic expressions onto the more general case of existing $N_{\rm r}$ relaxing and $N_{\rm p}$ pairs of propagating generalized hydrodynamic and kinetic collective excitations, $N_{\rm r} + 2N_{\rm p} = N_{\rm v}$. The amplitudes of the mode contributions $A^j(k)$, $B^j(k)$, $D^j(k)$ (mode strengths as named in [14]) from the collective modes can be estimated numerically from $G^j_{\alpha\beta}(k)$ in (2) for any k-point sampled in a real or computer experiment, that permits representation of the measured dynamical structure factors $S_{\alpha\beta}(k,\omega)$ in terms of separated mode contributions being extremely important for experimentalists.

The generalized expression for the dynamical structure factors (3) permits a comparison with the numerical approach of dispersion estimation of the collective excitations in binary liquids via the maxima positions of the current spectral functions $C_{\alpha\alpha}(k,\omega)$. These spectral functions according to (3) can be represented as

$$C_{\alpha\alpha}(k,\omega) \sim \sum_{j}^{N_{\rm r}} \frac{\omega^2}{k^2} A^j_{\alpha\alpha}(k)\frac{d_j(k)}{\omega^2+d_j^2(k)} + \sum_{j,\pm}^{N_{\rm p}} \frac{\omega^2}{k^2}\frac{B^j_{\alpha\alpha}(k)\sigma_j(k) + D^j_{\alpha\alpha}(k)(\omega \pm \omega_j(k))}{(\omega \pm \omega_j(k))^2+\sigma_j^2(k)}, \tag{4}$$

where the subindex α represents partial currents. Hence, in general, several relaxing and at least two pairs of propagating modes contribute to the shape of $C_{\alpha\alpha}(k,\omega)$ in binary liquids at any k-point. At $k \to 0$ the mode contributions from kinetic processes should tend to zero not more slowly than k^2, and only hydrodynamic collective modes with the only propagating branch of sound excitations contribute to the shape of $C_{\alpha\alpha}(k,\omega)$. This would explain why the two dispersion curves shown in figure 1 merge in the long-wavelength region into a single sound-like dispersion law.

Only the knowledge of all the important mode contributions $A^j(k)$, $B^j(k)$, $D^j(k)$ can establish the correspondence between the maxima positions of $C_{\alpha\alpha}(k,\omega)$ and the dispersion law of the propagating excitations. In [5] we have shown in a simple example of transverse dynamics in binary liquids how the main contributions to the transverse spectral functions $C_{\alpha\alpha}(k,\omega)$ behave as functions of the wavenumber. The case of longitudinal dynamics is much more complicated because of the strong influence of several relaxing processes due to thermal and mutual diffusion and structural relaxation, the amplitudes of which $A^j(k)$ can in general be of different sign beyond the hydrodynamic region. And only a theoretical analysis like the GCM approach, which permits consistent calculation of eigenmodes and mode contributions, can correctly produce the dispersion law in the whole k-range studied.

2.2. Details of molecular dynamics simulations

Computer simulations for Li_4Pb were performed in the standard microcanonical ensemble on a model system of 4000 particles in a cubic box subject to periodic boundary conditions at the temperature of 1085 K and mass density 3556.76 kg m^{-3}. The pair potentials $\Phi_{ij}(r)$, taken from [15], were the same as those used in previous studies of dynamics in Li_4Pb [1, 9]. The fourth-order Gear algorithm with the time step $\delta t = 1 \times 10^{-15}$ s was used for integrating the equations of motion. The production run was of 3×10^5 steps, and 11 k-points were sampled in the MD simulation. The smallest wavenumber reached in the simulations for Li_4Pb was $k_{\min} = 0.1414$ Å^{-1}.

Additional MD simulations were performed for an equimolar Lennard-Jones liquid at temperature $T = 116$ K and numerical density $n = 0.0182$ Å^{-3}. The parameters of the Lennard-Jones potentials were taken from [16] and corresponded to a KrAr mixture. Five production runs with a system of 864 particles in a cubic box were performed for mixtures with different mass ratio of components: starting from the KrAr system with mass ratio $m_{\mathrm{Kr}}/m_{\mathrm{Ar}} = 2.098$ we increased the mass ratio keeping the average mass constant in order to provide identical static properties for the five systems. The four other mass ratios were the following: $m_{\mathrm{h}}/m_{\mathrm{l}} = 4.65, 8.63, 12.39, 17.12$. The composition of the Lennard-Jones liquid mixture was the same in these five MD runs. In general 22 k-points in the range 0.1735–3.96 Å^{-1} were sampled in the MD simulations.

The time evolution of the basis dynamical variables was obtained from regular production runs over 3×10^5 time steps, while for the three lowest k-values, in order to obtain the desired convergence of the relevant static averages and time correlation functions, the five systems with different mass ratio were simulated over 2.1×10^6 time steps. For reducing the dimension of relevant quantities the following energy, mass, spatial and timescales were used in our simulations: $\epsilon = k_{\mathrm{B}}T$, $\mu = \bar{m}$, $\sigma = 5.764$ Å, $\tau = \sigma(\mu/\epsilon)^{1/2} = 4.598$ ps.

All the static and time correlation functions needed for estimation of matrix elements of the matrices of time correlation functions $\mathbf{F}(k, t)$ and their Laplace transforms $\tilde{\mathbf{F}}(k, z)$ were directly evaluated in computer simulations. The eigenvalues and eigenvectors of the generalized hydrodynamic matrix $\mathbf{T}(k)$ were calculated for each k-point sampled in molecular dynamics. Thus, in our GCM approach there were no fitting or free parameters.

3. Results

The main motivation for this study of spectra dependence on mass ratio in liquid binary mixtures was the GCM results of the collective dynamics in the liquid metallic alloy Li_4Pb obtained using the following eight-variable extended basis set:

$$\mathbf{A}^{(8)} = \{n_{\mathrm{t}}(k, t), n_{\mathrm{x}}(k, t), J_{\mathrm{t}}^{\mathrm{L}}(k, t), J_{\mathrm{x}}^{\mathrm{L}}(k, t), \varepsilon(k, t), \dot{J}_{\mathrm{t}}^{\mathrm{L}}(k, t), \dot{J}_{\mathrm{x}}^{\mathrm{L}}(k, t), \dot{\varepsilon}(k, t)\}, \tag{5}$$

where the hydrodynamic variables reflecting the slowest fluctuations in the binary liquid are: total density $n_{\mathrm{t}}(k, t)$, mass–concentration density $n_{\mathrm{x}}(k, t)$, total longitudinal mass-current $J_{\mathrm{t}}^{\mathrm{L}}(k, t)$ and energy density $\varepsilon(k, t)$. The variables with overdots correspond to the first time derivatives of the relevant fluctuations and are supposed to describe correctly more short-time processes than the hydrodynamic ones. The advantage of the GCM approach is in the consistent treatment of short-time processes in liquids which are orthogonal to the hydrodynamic ones. For example, the extended variable of longitudinal mass–concentration current $J_{\mathrm{x}}^{L}(k, t)$ is orthogonal to all hydrodynamic variables. This permits one to study kinetic collective processes in liquids which cannot be described by hydrodynamic theory. The choice of the eight-variable basis set (5) is defined by several factors:

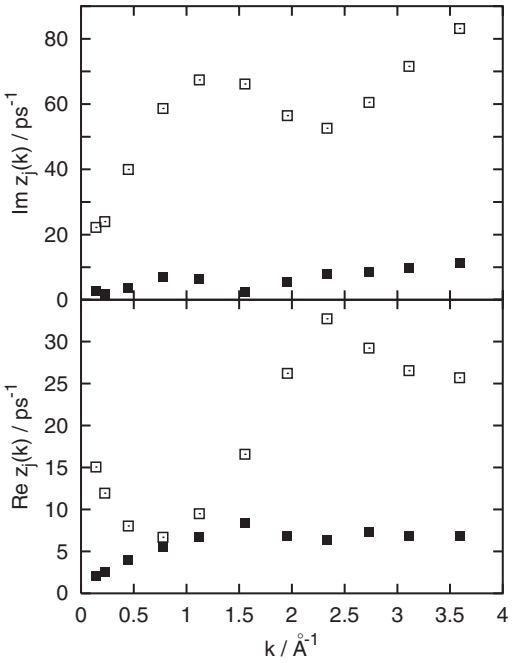

Figure 2. Propagating eigenmodes of liquid metallic alloy Li_4Pb at 1085 K obtained from the eight-variable (5) GCM treatment: frequency (imaginary parts) and damping coefficients (real parts) of propagating collective excitations. Open boxes correspond to high-frequency excitations, which in the long-wavelength region behave as kinetic optic phonon-like excitations.

(i) it must contain all hydrodynamic variables;
(ii) fluctuations of the total and mass–concentration currents and their time derivatives must be treated on the same level of approximation;
(iii) we may restrict our GCM treatment of short-time processes with the first time derivatives of the currents and energy, because our previous GCM studies of pure and binary liquids [5, 18] revealed that the second and third time derivatives of hydrodynamic variables in the basis set are responsible for additional kinetic excitations with very small lifetime, which can only marginally modify the eigenvalues obtained with the basis sets restricted by the first time derivatives of the currents and energy.

The eight-variable treatment (5) of the collective dynamics in Li_4Pb results in two pairs of complex-conjugated eigenvalues $z_j(k) = \sigma_j(k) \pm i\omega_j(k)$ in the whole range of wavenumbers studied. In figure 2 we show the real (damping coefficients) and imaginary (dispersion) parts of two branches of propagating eigenmodes in molten Li_4Pb. Four purely real eigenvalues $d_j(k)$ were obtained in the whole k-region studied. The three lowest relaxing modes $d_j(k)$ are shown in figure 3. One can see in figure 2 that the branches of propagating modes represent two processes well-separated in frequency. A detailed analysis of all dynamical eigenmodes in Li_4Pb can be found in [17]. Our main interest here is in the behaviour of the high-frequency branch in the long-wavelength region. In contrast to the results of the numerical analysis of MD-derived current–current spectral functions [9], where a merger of two branches in long-wavelength region was reported, we clearly observe in our theoretical GCM analysis the behaviour of the high-frequency branch in the small-k region similar to that of optic phonon-like excitations, which in liquids belong to kinetic collective excitations and have

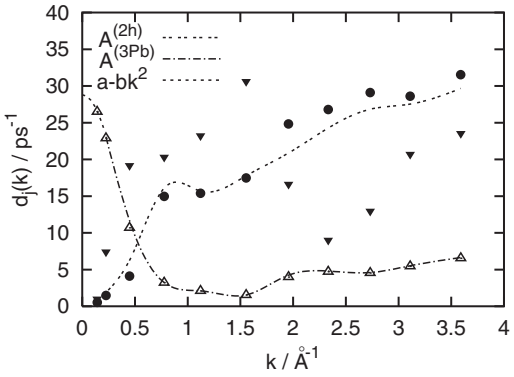

Figure 3. Three lowest real eigenmodes of liquid metallic alloy Li_4Pb at 1085 K obtained from the eight-variable (5) GCM treatment, which reflect generalized thermal diffusion (filled circles) and relaxing processes in light (filled triangles) and heavy (open triangles) subsystems. In the long-wavelength limit the filled triangles and filled circles tend to zero, and the open triangles correspond to a kinetic relaxing mode with expected asymptote $a - bk^2$ shown by the dashed curve. The results of separated GCM treatment of heat processes and partial dynamics of the heavy subsystem are shown by the double-dashed and dash–dotted curves, respectively.

finite damping coefficient in $k \to 0$ limit [7]. One can observe a systematic increase of the damping coefficient $\mathrm{Re}[z_{\mathrm{high}}(k)]$ in the long-wavelength region when $k \to 0$. The low-frequency branch of propagating excitations displays an interesting $\omega(k)$ dependence. It has a pronounced minimum at $k \approx 1.45$ Å^{-1}, which is at the main maximum location of the static structure factor $S_{\mathrm{PbPb}}(k)$. However, this low-frequency branch has another minimum in the dispersion law at $k \approx 0.25$ Å^{-1}. Such a minimum is never observed in binary liquid mixtures with comparable masses of species and concentrations. However, it is obvious that for the disparate-mass liquid mixtures there should exist a qualitative difference in the spectra of collective excitations between two cases of comparable concentrations and low concentration of the heavy component. In the latter case one could expect either the absence of the low-frequency branch in the spectrum of collective excitations in long-wavelength region with the high-frequency branch of light subsystem continuously transforming into hydrodynamic sound towards $k \to 0$, or continuous transformation of the low-frequency branch into a linear dispersion law with rather high slope when $k \to 0$. Namely, this scenario can explain the minimum in the dispersion law of the low-frequency branch at $k \approx 0.25$ Å^{-1}: if one assumed the linear dispersion at the smallest k-point of 0.1414 Å^{-1}, then we obtain the propagation speed of low-frequency excitations as $c = 1970$ m s^{-1}, which is very close to the hydrodynamic value of the speed of sound from [9]. Hence, if there exists a crossover from hydrodynamic to 'partial' character of the low-frequency branch around $k \approx 0.25$ Å^{-1}, then this can explain the observed features of low-frequency dispersion. The behaviour of the real parts of low-frequency excitations supports the fact that the smallest k-point reached in MD simulations is outside the hydrodynamic region and the k^2-dependence of hydrodynamic sound damping is not observed in the lower frame of figure 2. However, there exists a rather wide region, 0.15 Å$^{-1} < k < 1.5$ Å^{-1}, in which the real parts of the low-frequency branch behave almost linearly with k, which is in agreement with our previous GCM studies of generalized sound excitations in metallic Pb [18] and semimetallic Bi [19], for which the damping of generalized sound excitations increased linearly with k beyond the hydrodynamic region.

In figure 3 we show the k-dependence of three main relaxing processes, which reflect heat relaxation (filled circles) and relaxing processes in light (filled triangles) and heavy (open

triangles) subsystems for $k > 0.25$ Å^{-1}. The way we identified the k-dependence of each relaxing process among the four real eigenvalues was the same as we used in our previous study of the liquid Lennard-Jones mixture KrAr [20], which consists of applying separated subsets of dynamical variables within the GCM approach. Figure 3 shows, by the double-dash and dash–dotted curves, the behaviour of the lowest real eigenvalues, obtained from the 2×2 and 3×3 generalized hydrodynamic matrices generated on the separated sets $\mathbf{A}^{(2h)} = \{h(k,t), \dot{h}(k,t)\}$ ($h(k,t)$ is a dynamical variable of heat density, which is orthogonal to both dynamical variables of total and mass–concentration density fluctuations) and $\mathbf{A}^{(3Pb)} = \{n_{Pb}(k,t), J^{L}_{Pb}(k,t), \dot{J}^{L}_{Pb}(k,t)\}$, respectively. It is clearly seen that for $k > 0.25$ Å^{-1} the relaxing process shown by open triangles is completely defined by the heavy subsystem of Pb atoms. For smaller wavenumbers this relaxing mode continuously changes into a kinetic relaxing process with a finite relaxation time in the long-wavelength limit and which should have an asymptote $d_{kin} = a - bk^2$ for $k \to 0$ similar to that observed for other pure and binary liquids [18, 20] (the quantities a and b are defined by the kinematic viscosity D_L). The filled triangles in figure 3 in the long-wavelength region correspond to the relaxing process of mutual diffusion. With increasing wavenumbers this relaxing process describes solely the light subsystem of Li atoms: a well-pronounced minimum of this dependence $d(k)$ at $k \approx 2.35$ Å^{-1} is located right at the position of the main peak of the partial static structure factor $S_{LiLi}(k)$.

All the collective propagating and relaxing modes shown in figures 2 and 3 contribute to the shape of the dynamical structure factors $S_{\alpha\beta}(k,\omega)$ with k-dependent mode amplitudes according to (3). Here we will focus on the symmetric mode contributions $B^{j}(k)$ coming from the high- and low-frequency propagating excitations in Li_4Pb to the shape of dynamical structure factors $S_{tt}(k,\omega)$ and $S_{LiLi}(k,\omega)$ in order to explain the results obtained in the earlier studies of dispersion of collective excitations in Li_4Pb [1, 9] and which were based solely on numerical analysis of partial spectral functions $S_{\alpha\alpha}(k,\omega)$ and $C_{\alpha\alpha}(k,\omega)$, $\alpha = \mathrm{Li}, \mathrm{Pb}$. In figure 4(a) are shown the symmetric amplitudes $B^{j}_{tt}(k)$ obtained in our eight-variable GCM analysis of the collective dynamics in molten Li_4Pb, which reflect contributions from the two propagating branches to the dynamical structure factor $S_{tt}(k,\omega)$ defined by the hydrodynamic variables of total density. It is important that for $S_{tt}(k,\omega)$ there exist analytical hydrodynamic results [21], which estimate the symmetric contribution $B^{sound}(k \to 0)$ coming from hydrodynamic sound excitations at the value γ^{-1}. Our estimate for the ratio of specific heats in molten Li_4Pb is $\gamma = 1.15$ (see [17]); hence the contribution from the sound excitations to the $S_{tt}(k,\omega)$ in the long-wavelength limit should be $\approx$0.87. In figure 4(a) one can see how the role of different propagating modes changes towards the long-wavelength region: in the region 0.5 Å$^{-1} < k < 1.8$ Å^{-1} the main contribution to the side peaks of $S_{tt}(k,\omega)$ comes from the high-frequency branch, while for smaller wavenumbers there exists a crossover in the main contributions from the two propagating processes: the mode contribution from the kinetic high-frequency branch tends to zero, while the one from generalized sound excitations increases up to its hydrodynamic value of $\approx$0.87 when $k \to 0$. In order to make a direct comparison with the results by Bosse *et al* [1] we show in figure 4(b) the mode contributions $B^{j}(k)$ to the partial dynamical factor of the light component $S_{LiLi}(k,\omega)$. Again, there exists a crossover in the mode contributions from two propagating processes in the region $k \approx 0.3$ Å^{-1}, which means that even the partial correlations of the light component reflect in the long-wavelength region solely hydrodynamic sound excitations, but not some 'fast sound' excitations. Our GCM results for Li_4Pb permit us to explain the 'fast sound' observation [1] as a crossover in the mode contributions from the high- and low-frequency branches to the partial spectral functions, while the correct dispersion and damping of the propagating eigenmodes in the long-wavelength region behave as shown in figure 2. The large mass ratio $R \approx 30$ in the case of Li_4Pb is responsible for a large frequency gap between the two branches of high- and

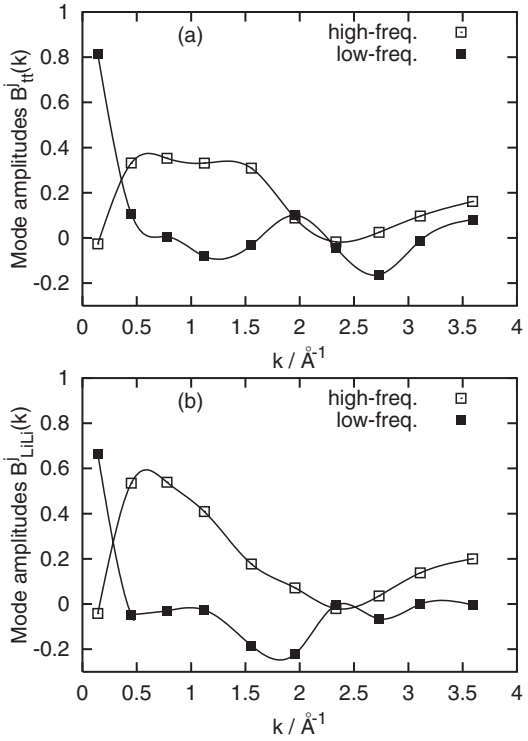

Figure 4. Amplitudes of symmetric mode contributions $B^j(k)$ from high- and low-frequency propagating excitations to the shape of the dynamical structure factor 'total density–total density' $S_{tt}(k,\omega)$ (a) and the partial dynamical structure factor of the light component $S_{\mathrm{LiLi}}(k,\omega)$ (b) for liquid Li_4Pb. The partial dynamical structure factor $S_{\mathrm{LiLi}}(k,\omega)$ was used in [1] for estimation of the 'fast sound' dispersion. Open and filled boxes correspond to the same branches as in figure 2. Solid curves are the spline interpolation.

low-frequency excitations and an extended range of 'partial' behaviour of the two branches towards longer wavelengths. These last statements we will discuss in more detail in an example of Lennard-Jones liquid mixtures.

For comparison with the spectrum of a molten alloy with disparate mass discussed above, we show in figure 5 the spectrum of the propagating collective modes in a Lennard-Jones equiatomic liquid with a small mass ratio. The eight-variable GCM analysis (5) of the collective dynamics in liquid KrAr at 116 K yields three branches of propagating excitations: two branches of propagating density fluctuations (open and filled boxes in figure 5) and one corresponding to low-frequency heat waves ('plus' symbols in figure 5) in the liquid mixture. For $k > 0.5$ Å^{-1} the two branches shown by the open and filled boxes have nearly the same damping coefficients, while in the region of small wavenumbers the branch shown with open boxes tends to a finite nonzero damping coefficient, that is a specific feature of kinetic collective modes. The branch shown by filled boxes has an almost linear dispersion law in the long-wavelength region $\omega(k) = ck$ with the slope $c = 808$ m s^{-1}, while the corresponding real parts of the eigenvalues for $k < 0.3$ Å^{-1} behave almost proportional to k^2. In [7] we identified the two branches in liquid KrAr in the small-k region as generalized sound and optic phonon-like collective excitations. One can compare the two dispersion curves obtained by the GCM approach (shown by open and filled boxes in figure 5) with the results of numerical

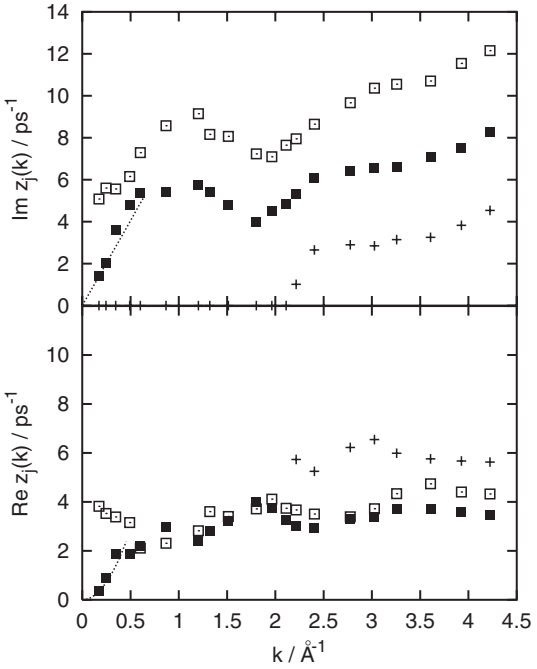

Figure 5. Complex eigenmodes of equiatomic Lennard-Jones KrAr liquid at 116 K: frequency (imaginary part) and damping coefficients (real parts) of the propagating collective excitations. Open boxes correspond to kinetic optic-like excitations, filled boxes to generalized sound excitations, and 'plus' symbols to low-frequency heat waves.

estimation of the dispersion from the maxima positions of the partial current spectral functions $C_{\alpha\alpha}(k,\omega)$, $\alpha =$ Kr, Ar: the main difference is observed in the long-wavelength region, where the high-frequency branch in figure 1 does not tend to a finite nonzero frequency at $k \to 0$. Such a discrepancy is evidence of an inadequacy of the numerical estimation of the dispersion of the high-frequency branch from the maxima positions of the partial current spectral functions in the long-wavelength region.

In order to understand in detail the formation of high-frequency collective excitations in liquid mixtures with disparate mass we show in figure 6 the behaviour of the high-frequency branches in an equimolar Lennard-Jones liquid mixture with different mass ratio, but the same mass density and interatomic potentials. The results of the 8×8 eigenvalue problem for two branches of propagating excitations in the reference KrAr liquid mixture with mass ratio $R = 2.098$ are shown by 'plus' symbols. The results for propagating excitations obtained by solving the 3×3 eigenvalue problem for the generalized hydrodynamic matrix constructed only on the partial dynamical variables $\mathbf{A}^{(3\alpha)} = \{n_\alpha(k,t),\, J^{\mathrm{L}}_\alpha(k,t),\, j^{\mathrm{L}}_\alpha(k,t)\}$, where α corresponds to heavy and light component in the mixture, are shown by dashed and solid lines, respectively. This means that the branches obtained within the general eight-variable treatment (shown by symbols) in the region of intermediate and large wavenumbers correspond well to the 'partial' character of the collective dynamics, while in the longer-wavelength region a treatment in terms of hydrodynamic fluctuations and processes orthogonal to them is necessary. In figure 6, the dispersion of the high-frequency branch in the Lennard-Jones liquid mixture for mass ratios $R = 4.65, 8.63, 17.12$ are shown by asterisks, open boxes and filled boxes, respectively. The general tendency with increasing mass ratio is twofold: (i) increasing the frequency of the

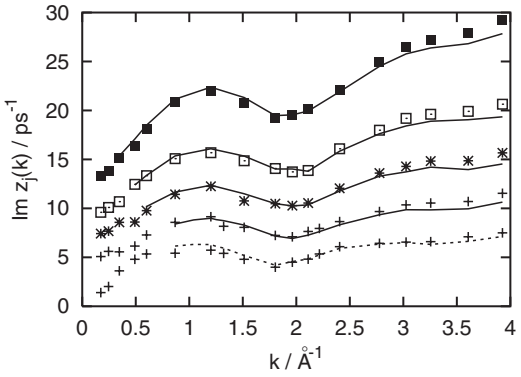

Figure 6. Dispersion curves obtained from the eight-variable GCM treatment $\mathbf{A}^{(8)}$ for two branches of propagating excitations in liquid KrAr (plus symbols) and high-frequency branches for the mass ratio: 4.65 (asterisks), 8.63 (open boxes), 17.12 (filled boxes). The solid lines correspond to propagating eigenvalues obtained from the three-variable $\mathbf{A}^{(3\alpha)}$ treatment of the light subsystem, while the dashed line reflects the branch of the Kr subsystem in KrAr liquid. The solid and dashed lines are shown only in regions of wavenumbers where a good correlation with the eight-variable results (symbols) was observed. The change in the correlation region provides evidence that the range of 'partial' character of branches extends towards smaller wavenumbers against increasing mass ratio.

optic-like branch, and (ii) extending the range of the 'partial' character of the dynamics towards the region of small wavenumbers. For all studied values of R we observed the typical behaviour of the high-frequency branch, as for optic phonon-like excitations. In the next section we will discuss the damping coefficient of optic-like modes and its dependence on the mass ratio.

4. Discussion

We will discuss the results obtained using a separated treatment of processes in the long-wavelength region connected with slow mass–concentration fluctuations and fast mutual current fluctuations orthogonal to them. Let us consider a three-variable basis set:

$$\mathbf{A}^{(3x)} = \{n_{\mathrm{x}}(k,t),\, J_x^{\mathrm{L}}(k,t),\, \dot{J}_x^{\mathrm{L}}(k,t)\}. \tag{6}$$

Here the only hydrodynamic variable is

$$n_{\mathrm{x}}(k,t) = \frac{1}{\bar{m}}\{m_1 x_2 n_1(k,t) - m_2 x_1 n_2(k,t)\} \equiv \frac{m_1 m_2}{\bar{m}^2} n_{\mathrm{c}}(k,t), \tag{7}$$

which describes the slowest mass–concentration fluctuations in a binary liquid;

$$n_\alpha(k,t) = \frac{1}{\sqrt{N}} \sum_{i=1}^{N_\alpha} \mathrm{e}^{\mathrm{i}\mathbf{k}\mathbf{r}_{\alpha,i}(t)}, \qquad \alpha = 1, 2,$$

are the ordinary variables of partial densities, and m_α and $x_\alpha = m_\alpha c_\alpha/\bar{m}$ are the atomic masses and mass–concentration factors, respectively. The reason for introducing the dynamical variable $n_{\mathrm{x}}(k,t)$ in the form (7) is that it is proportional to the ordinary concentration density $n_{\mathrm{c}}(k,t)$ and at the same time it is connected to the longitudinal component of the mass–concentration current $J_{\mathrm{x}}^{\mathrm{L}}(k,t)$ (introduced in [5]) by a simple relation:

$$\frac{\partial n_{\mathrm{x}}}{\partial t} = \frac{\mathrm{i}k}{\bar{m}} J_{\mathrm{x}}^{\mathrm{L}}(k,t). \tag{8}$$

The mass–concentration density $n_{\rm x}(k,t)$ is a hydrodynamic variable and along with the dynamical variables of total density $n_{\rm t}(k,t)$, total mass-current density $\mathbf{J}_{\rm t}(k,t)$ and energy density $\varepsilon(k,t)$ it is commonly used for the hydrodynamic description of any binary system in the liquid state. It was shown in [5] that $\mathbf{J}_{\rm x}(k,t)$ is an orthogonal dynamical variable to $\mathbf{J}_{\rm t}(k,t)$, and its real space representation reflects the out-of-phase motion for neighbours of different type.

In the basis set (6) the $\dot{J}_x^{\rm L}(k,t)$ is the first time derivative of the longitudinal mass–concentration current. The only hydrodynamic variable in this basis set is $n_{\rm x}(k,t)$, while the two other dynamical variables describe shorter-time fluctuations. The basis set (6) corresponds to the same level of short-time fluctuation treatment as was applied in the analytical study of the transverse dynamics in binary liquids [5, 6]. Solving analytically the eigenvalue problem for the 3×3 generalized hydrodynamic matrix $\mathbf{T}(k)$ in the long-wavelength limit, one obtains the following dynamical eigenmodes: (i) the lowest eigenvalue is purely real and simply reads

$$d(k) = D_{12}k^2, \tag{9}$$

where D_{12} is the mutual diffusion coefficient [21] taking into account that no other slow processes contribute to the shape of $F_{xx}(k,t)$ within our three-variable model; (ii) a complex-conjugated pair of eigenvalues, which tend in the long-wavelength limit to some constant values:

$$z^{\pm}(k\to 0) = \Gamma(k) \pm {\rm i}\sqrt{\omega^2_{J_{\rm x}J_{\rm x}}(k) - \Gamma^2(k)}, \tag{10}$$

where

$$\Gamma(k) = \frac{\bar{m}D_{12}\omega^2_{J_{\rm x}J_{\rm x}}(k)S_{xx}(k)}{2x_1x_2k_{\rm B}T} \equiv \frac{m_1m_2D_{12}\omega^2_{J_{\rm x}J_{\rm x}}(k)S_{cc}(k)}{2c_1c_2\bar{m}k_{\rm B}T} \tag{11}$$

is the damping of optic phonon-like excitations (mass–concentration waves) in the limit $k\to 0$ and the imaginary part of $z^{\pm}(k)$ represents their frequency. The quantity

$$\omega^2_{J_{\rm x}J_{\rm x}}(k) = \frac{\langle \dot{J}^{\rm L}_{\rm x}(-k)\dot{J}^{\rm L}_{\rm x}(k)\rangle}{\langle J^{\rm L}_{\rm x}(-k)J^{\rm L}_{\rm x}(k)\rangle}, \tag{12}$$

is in fact the ratio of the fourth and second frequency moments of the dynamical structure factor $S_{xx}(k,\omega)$ in the standard definitions of [22], and the static average $\langle \dot{J}^{\rm L}_{\rm x}\dot{J}^{\rm L}_{\rm x}\rangle$ tends to a constant in the $k\to 0$ limit.

Let us analyse the damping $\Gamma(k\to 0)$ of optic phonon-like excitations in the long-wavelength region. There is very rich physics hidden in expressions (10) and (11). In [7] we focused on two main processes which can suppress the propagation of optic phonon-like excitations in binary liquids: the high mutual diffusivity D_{12} and the demixing tendency, when the atoms are surrounded mainly by like ones and $S_{xx}(k\to 0)$ takes large values. Let us look now at the damping coefficient of long-wavelength optic excitations from the point of view of mass ratio $R = m_{\rm h}/m_{\rm l}$ dependence, where $m_{\rm h} = m_{\rm Kr} + \delta$ and $m_{\rm l} = m_{\rm Ar} - \delta$ are the heavy and light masses in the equimolar mixture. Note that $m_{\rm h}$ and $m_{\rm l}$ tend to a constant and zero, respectively. Among the factors which determine the mass-ratio dependence of the damping coefficient Γ (10) of the long-wavelength optic-like excitations are:

(i) a factor $m_{\rm h}m_{\rm l} \equiv m^2_{\rm h}/R$ in the numerator, which is a decaying to zero function of R;
(ii) a quantity $\omega^2_{J_{\rm x}J_{\rm x}}(R)$, which we can calculate numerically in MD simulations via the definition (12); and
(iii) the mutual diffusivity $D_{12}(R)$ for which we can use either analytical results known for the hard sphere systems [23, 24] or make some estimates from our MD simulations.

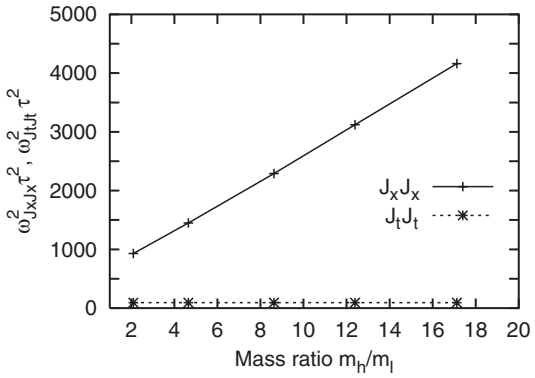

Figure 7. The dependence estimated in MD simulations of the quantities $\omega^2_{J_x J_x}(k)$ and $\omega^2_{J_t J_t}(k)$ on the mass ratio for an equimolar KrAr mixture for the smallest wavenumber of 0.1735 Å^{-1}. These quantities correspond to the square of the 'bare' frequencies of optic-like ('plus' symbols) and acoustic (asterisks) excitations at $k = k_{\min}$. The timescale is $\tau = 4.598$ ps.

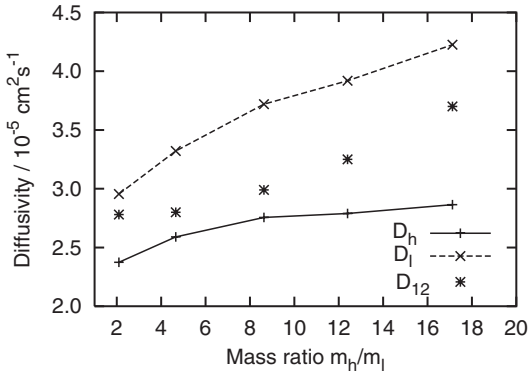

Figure 8. Estimated self-diffusion coefficients for the light $D_{\rm l}$ and heavy $D_{\rm h}$ component in the five Lennard-Jones systems with different mass ratio (shown by line-connected symbols). The coefficient of the k^2 dependence of the lowest relaxing mode $d_x(k)$, which defines mutual diffusivity in the binary liquids, is shown by asterisks.

In figure 7 we show that the quantity $\omega^2_{J_x J_x}(k_{\min})$ obtained directly in MD simulations depends linearly on the mass ratio R. This quantity, in fact, is the square of the frequency of 'bare' optic-like excitations at $k = k_{\min}$. Due to the interaction with the relaxing process of mutual diffusivity, the frequency of the optic-like modes reduces from its 'bare' value according to (10). A similar quantity $\omega^2_{J_t J_t}(k_{\min})$, which is the square of the frequency for 'bare' acoustic excitations, does not change with the mass ratio R; that is correct because this quantity is defined solely by the total density, which is constant. The linear dependence of $\omega^2_{J_x J_x}(k \to 0)$ on the mass ratio implies that its product with $m_{\rm h} m_{\rm l}$ should tend to a constant at large R. Hence, the leading dependence of the damping Γ on the mass ratio R should be due to the mutual diffusivity $D_{12}(R)$. We have calculated the self-diffusion coefficients of the light $D_{\rm l}(R)$ and heavy $D_{\rm h}(R)$ subsystems for the five Lennard-Jones liquid mixtures with the same total density from the linear asymptote of mean-squared displacements (see figure 8). Both self-diffusion coefficients increase with the mass ratio R. In figure 8, the coefficient of the k^2 dependence for the lowest relaxing eigenvalues in the long-wavelength region (see equation (9)), which

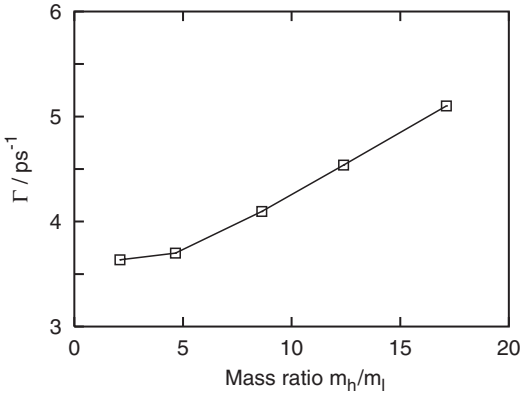

Figure 9. Dependence of the damping coefficient Γ (10) for optic phonon-like modes within the three-variable treatment $\mathbf{A}^{(3x)}$ (open boxes connected by solid line) on mass ratio for the smallest wavenumber of 0.1735 Å^{-1}.

correspond to the process of mutual diffusion, are shown by asterisks. It should be mentioned that D_{12} obtained in this way may have some, presumably small, contribution from the thermal processes (see [21]). The mutual diffusivity $D_{12}(R)$ takes values between both self-diffusion coefficients as it should, and changes slowly for small mass ratio, while it displays an almost linear with R behaviour at large mass ratio.

In figure 9 we show how the damping of the optic-like modes $\Gamma(k_{\min})$, evaluated within the three-variable model (10) at the smallest k-point sampled in our MD simulations of Lennard-Jones mixtures, increases against the mass ratio in agreement with our arguments. It is remarkable that this dependence is very similar to the dependence of $D_{12}(R)$ in figure 8 as follows from expression (11). Hence, our analysis has shown that the damping coefficient of long-wavelength optic-like excitations in liquid mixtures increases with mass ratio R.

More interesting is the dependence of the damping of optic-like excitations on molar composition in the liquid mixtures, which is more difficult to study because all the static structural properties will change. Such a GCM study of the concentration dependence of spectra of collective excitations in binary liquids is in progress and will be presented elsewhere.

5. Conclusions

We summarize this study with the following remarks.

(1) The spectrum of propagating collective excitations in liquid metallic alloy Li_4Pb obtained from the parameter-free eight-variable GCM treatment consists of two branches of collective excitations. The high-frequency branch in the long-wavelength region shows the typical behaviour of overdamped optic phonon-like excitations.

(2) We have shown how the mode contributions from the high- and low-frequency propagating excitations to the two dynamical structure factors of main interest behave in a wide region of wavenumbers. It follows from the theoretical GCM treatment of the longitudinal dynamics in molten Li_4Pb, that the kinetic high-frequency excitations identified in the long-wavelength region as optic phonon-like modes do not contribute to the partial dynamical structure factor of the light component when $k \to 0$, while the main contribution to the Brillouin side peak should be due to sound excitations in the long-wavelength limit. Hence, the 'fast sound' phenomenon reported in [1] can be explained by our GCM results

as follows: because of the huge mass ratio in Li_4Pb the 'partial' character of the branches of the collective excitations is extended down to approximately 0.5 $Å^{-1}$; for smaller wavenumbers a crossover to hydrodynamic behaviour takes place, which is reflected in the vanishing contribution from the high-frequency kinetic branch and the increasing contribution from the sound excitations to the partial dynamical structure factor $S_{\mathrm{LiLi}}(k, \omega)$. Such a crossover in mode contributions to $S_{\mathrm{LiLi}}(k, \omega)$ causes a 'fast sound'-like dispersion curve when it is estimated numerically from the Brillouin peak position of $S_{\mathrm{LiLi}}(k, \omega)$;

(3) In order to clarify the tendency in the frequency and damping coefficients for optic-like excitations in disparate mass mixtures we performed a GCM study of collective dynamics in Lennard-Jones liquid mixtures with different mass ratio. Our analytical three-variable analysis shows that the frequency and damping coefficient of the long-wavelength optic-like excitations increase with the mass ratio R.

Acknowledgment

IM thanks the Fonds zur Förderung der wissenschaftlichen Forschung (Austria) for financial support under Project No. P15247.

References

[1] Bosse J, Jacucci G, Ronchetti M and Schirmacher W 1986 *Phys. Rev. Lett.* **57** 3277
[2] de Schepper I M, Cohen E G D, Bruin C, van Rijs J C, Montfrooij W and de Graaf L A 1998 *Phys. Rev.* A **38** 271
[3] Mryglod I M, Omelyan I P and Tokarchuk M V 1995 *Mol. Phys.* **84** 235
[4] Bryk T, Mryglod I and Kahl G 1997 *Phys. Rev.* E **56** 2903
[5] Bryk T and Mryglod I 2000 *Phys. Rev.* E **61** 2088
[6] Bryk T and Mryglod I 2000 *J. Phys.: Condens. Matter* **12** 6063
[7] Bryk T and Mryglod I 2002 *J. Phys.: Condens. Matter* **14** L445
[8] Enciso E, Almarza N G, Dominguez P, Gonzalez M A and Bermejo F J 1995 *Phys. Rev. Lett.* **74** 4233
[9] Fernandez-Perea R, Alvarez M, Bermejo F J, Verkerk P, Roessli B and Enciso E 1998 *Phys. Rev.* E **58** 4568
[10] Anento N and Padro J A 2001 *Phys. Rev.* E **64** 021202
[11] Gonzalez D J, Gonzalez L E, Lopez J M and Stott M J 2003 *Europhys. Lett.* **62** 42
[12] Mryglod I 1998 *Condens. Matter Phys.* **1** 753
[13] Cohen C, Sutherland J W H and Deutch J M 1971 *Phys. Chem. Liq.* **2** 213
[14] March N H and Tosi M P 1984 *Coulomb Liquids* (London: Academic)
[15] Jacucci G, Ronchetti M and Schirmacher W 1984 *Condensed Matter Research Using Neutrons* ed S W Lovesey and R Scherm (New York: Plenum)
[16] Gardner P J, Heyes D M and Preston S R 1991 *Mol. Phys.* **73** 141
[17] Bryk T and Mryglod I 2004 *Condens. Matter Phys.* **7** 285
[18] Bryk T and Mryglod I 2001 *Phys. Rev.* E **63** 051202
[19] Bryk T and Mryglod I 2000 *J. Phys.: Condens. Matter* **12** 3543
[20] Bryk T and Mryglod I 2004 *Condens. Matter Phys.* **7** 15
[21] March N H and Tosi M P 1976 *Atomic Dynamics in Liquids* (London: Macmillan)
[22] Hansen J-P and McDonald I R 1986 *Theory of Simple Liquids* (London: Academic)
[23] van den Berg H P and Hoheisel C 1990 *Phys. Rev.* A **42** 3368
[24] Tankeshwar K 1995 *J. Phys.: Condens. Matter* **7** 9715